Supporting Information. Shaw, C.L., S.R. Hall, E.P. Overholt, C.E. Cáceres, C.E. Williamson, and M.A. Duffy. 2020. Shedding light on environmentally transmitted parasites: lighter conditions within lakes restrict epidemic size. Ecology.

APPENDIX S1

Section S1. Additional lake transparency methods

In this section, we explain how we calculated metrics of light exposure and the index of lake transparency in the main text.

Incubation experiment: Within-lake light attenuation
Diffuse attenuation coefficients (k_{d320} and k_{dPAR}) measure light attenuation in water, accounting for the contribution of both the dissolved and particulate substances. Diffuse attenuation coefficients were calculated from profiles generated by a submersible radiometer (BIC 2104, Biospherical Instruments, Inc., San Diego, CA). We use these values to estimate the percentage of ambient light (320 nm UV and PAR) remaining at the incubation depths of 0.5 and 2 m in each lake (see equation S1; Rose et al. 2009).

$$\% \text{ Light remaining} = e^{-\text{depth} * kdPAR} * 100\% \quad (S1)$$

We measured diffuse light attenuation coefficients in lakes with the experimental incubations in July and August, but not in November. Diffuse light attenuation in Beaver Dam Lake was not measured in July. In the analysis, we used diffuse light attenuation coefficients from the relevant month if possible. Otherwise, we used the diffuse light attenuation coefficient from the proximate month measured. To justify, light attenuation coefficients did not change significantly through autumn in a linear mixed effects model with month as a fixed effect, and lake and year as random effects (k_{d320}: Likelihood Ratio Test (LRT)=1.24, P=0.27; k_{dPAR}: LRT=0.25, P=0.62).

Incubation experiment: Ambient Light
During each incubation, a radiometer (Model 2104RL; Biospherical Instruments, Inc. San Diego, California, USA) measured ambient incident radiation integrated over 3-minute time intervals. The instrument was deployed at the Greene Sullivan State Forest ranger station located 10 miles from all experimental lakes. We report both the maximum 320 nm and PAR irradiances within a 3-minute time interval and the cumulative irradiances (summed over the deployment) while the incubations were deployed in each lake. Due to time needed for deployment and recovery of the incubations, light measurements are slightly different for each lake (Table S1, Table S2).

Table S1. Light and temperature conditions at incubation depths and incident light conditions above the water surface during experimental incubations. Diffuse light attenuation was not measured in November, and diffuse light attenuation in Beaver Dam was not measured in July. Canvasback was not included in the November incubation.

	% PAR remaining at incubation depths: 0.5 m, 2.0 m		Water temperature (°C) at 0.5 m (shallower, lighter), 2.0 m (deeper, darker)			Cumulative incoming light, UV (at 320 nm, KJ/m^2) and PAR ($W/m^2 \times 10^7$)		
Lake	Jul	Aug	Jul	Aug	Nov	Jul	Aug	Nov
Airline[1]	85.6%, 53.8%	84.0%, 49.9%	28.7, 28.6	28.4, 28.4	18.1, 18.1	29.23 3.749	18.61 2.181	11.01 1.734
Beaver Dam[2]		71.9%, 26.7%	28.6, 27.9	27.7, 27.3	17.1, 17.1	29.93 3.820	17.00 2.018	10.72 1.688
Canvasback[3]	86.4%, 55.8%	84.9%, 51.9%	29.4, 28.9	28.4, 28.4		30.46 3.887	17.88 2.107	
Goodman[1]	83.7%, 49.0%	72.0%, 26.9%	28.6, 28.1	27.7, 27.7	17.3, 17.3	30.41 3.881	18.31 2.151	11.06 1.742
Midland[2]	64.5%, 17.3%	53.8%, 8.4%	28.7, 28.6	28.1, 28.1	16.8, 16.8	30.18 3.842	17.56 2.075	10.82 1.703

[1] Greene-Sullivan State Forest, Greene County, IN; [2] Hillenbrand Fish and Wildlife Area, Greene County, IN; [3] Sullivan County, IN.

Table S2. Time of deployment and recovery of incubation set up.

Lake	July	August	November
Airline	7/20/16 12:30pm – 7/25/16 8:20am	8/15/16 11:15am – 8/20/16 8:10am	10/31/16 10:00am – 11/5/16 8:46am
Beaver Dam	7/20/16 11:00am – 7/25/16 7:45am	8/15/16 2:30pm – 8/20/16 7:00am	10/31/16 11:30am – 11/5/16 8:08am
Canvasback	7/20/16 3:30pm – 7/25/16 9:00am	8/15/16 1:30pm – 8/20/16 7:30am	
Goodman	7/20/16 1:45pm – 7/25/16 8:40am	8/15/16 12:30pm – 8/20/16 8:30am	10/31/16 9:30am – 11/5/16 9:01am
Midland	7/20/16 9:20am – 7/25/16 7:20am	8/15/16 2:30pm – 8/20/16 6:30pm	10/31/16 11:00am – 11/5/16 7:45am

Analysis of field survey: Index of lake transparency

Like diffuse attenuation coefficients above, dissolved absorption coefficients quantify the attenuating properties of dissolved substances in water, but they do not incorporate the attenuating properties of particulate substances in water samples. Hence, these values can be lower than the dissolved absorption coefficients. In this study we measured the dissolved absorption coefficient for 320 nm UV (a_{d320}). Dissolved absorption coefficients are calculated as equation S2.

$$a_{d\lambda} = 2.303D/r \qquad (S2)$$

where D is the absorbance of the water sample at wavelength (λ) defined as $D=\log_{10}(I_0/I)$ where I_0 is the incident light intensity, and I is the light remaining after passing through the sample, r is the pathlength in the spectrophotometer (in cm), and 2.303 converts base e to base 10 logarithms (Kirk 1993). To measure a_{d320}, we collected epilimnetic water samples and filtered them with pre-combusted Whatman glass fiber filters (GF/F). The filtrates were kept refrigerated until analysis by spectrophotometry (Shimadzu UV⁄ Visible UV-1650 PC Spectrophotometer). For the field survey, in 2014, we collected water samples from each lake throughout the season; in 2015 water samples were collected in July and in October, whereas in 2016 water samples were collected in August only. For years with more than one water sample, a_{d320} was averaged.

Diffuse attenuation coefficients for UV (k_{d320}) were not measured in all of our study lakes in every year. Hence, we estimated k_{d320} when not measured using its relationship with the dissolved absorption coefficient (a_{d320}) for UV (Figure S1, Equation S3).

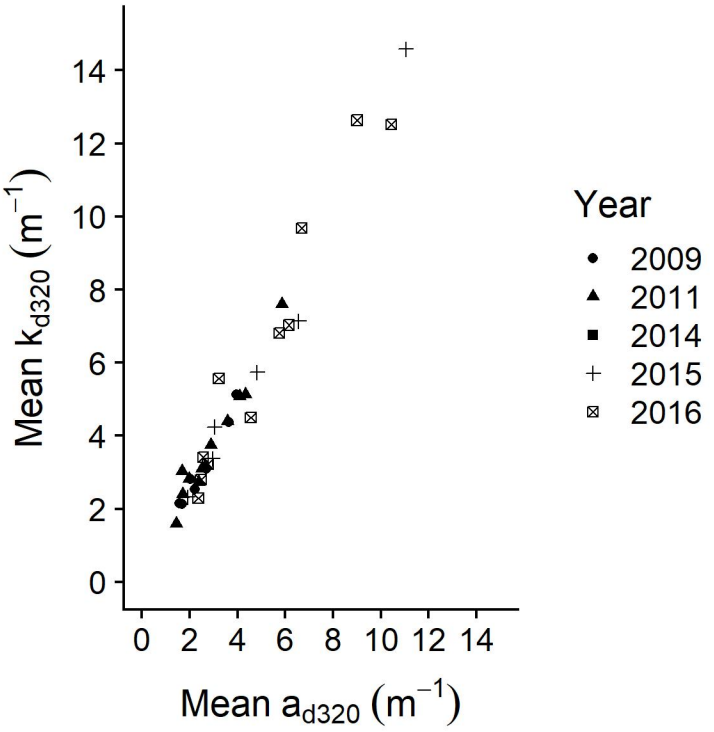

Figure S1. Mean values of a_{d320} and k_{d320} in lakes where both were measured in a given year were correlated (r^2=0.963, P<0.001).

The strong linear relationship (equation S3, Fig S1) used to estimate k_{d320} values was:

$$\text{Estimated } k_{d320} = -0.07055 + 1.27437 * a_{d320} \qquad (S3)$$

With these k_{d320} estimates, we then calculated the depth of 1% of remaining 320nm UV light (by solving for depth in parameterized equation S1). We used this depth as our index of lake transparency.

Section S2. Additional experimental notes and procedures

Lost Samples
We lost uncovered vials of *Metschnikowia* spores at 2 m in Goodman Lake in the November incubation. We also do not have data for a vial of *Pasteuria* from Canvasback Lake in the covered treatment at 0.5 m in July, a vial of *Pasteuria* from Canvasback Lake that was exposed to light at 2 m in August, and a vial of *Metschnikowia* from Midland Lake that was exposed at 2 m in November. In addition, we lost physical access to Canvasback Lake during the fall, so this lake was also left out of the November incubation.

Notes on Daphnia *maintenance*
In July, animals were maintained in the Hall Lab at Indiana University, and in August and November, animals were maintained in the Duffy Lab at the University of Michigan. Due to differences in lab methods for *Daphnia* care, in the Hall lab, *Daphnia* were fed 1 mg

Ankistrodesmus falcatus per liter on the day of exposure and 2 mg *Ankistrodesmus* per liter every day after exposure, and in the Duffy lab, *Daphnia* were fed 1x10^6 cells (1.63 mg L^{-1}) of *Ankistrodesmus* every day. All levels of food are considered 'high' for *Daphnia*.

Notes on experimental take down
We maintained *Daphnia* only until infection could be ascertained, as described below.

July incubation: No new *Metschnikowia* infections were observed after the 14th day post infection, so all animals were diagnosed by the 16th day post infection. For *Pasteuria*, some animals had discernable infections as early as 14 days post infection, and they were taken down. Remaining animals were checked every other day until 20 days post infection, at which point all were diagnosable as infected or uninfected.

August incubation: Late-stage *Metschnikowia* infections could be discerned on the 10th day post infection, and remaining animals were taken down 13 days post infection at which point 4 additional animals were found to have *Metschnikowia*, but the others were clearly uninfected. Two questionable animals were maintained and found later to have been infected with *Pasteuria*. These animals and two more which had been noted to be questionable at take down were classified as uninfected for the analysis. However, if these animals had been counted as infected, there would be no qualitative change in the results presented here. Contamination was likely due to movement of spores during an early water change. *Pasteuria* infections were discernable 14 days post infection. Like in the July incubation, animals in the *Pasteuria* treatment that were clearly infected were taken down at or before 20 days post infection. However, even with examination under the microscope, 53 (of 590 total *Pasteuria*-exposed animals) could not be confidently diagnosed at this date; these were kept until 29 days post-infection, at which point 16 were clearly infected. If the animals which were classified as infected after the 20 day mark had been classified instead as uninfected, there would be no change in the qualitative results reported here for the comparison between parasites or for the *Pasteuria* results.

November: For the November incubation, *Metschnikowia* infections were discernable by 11 days post infection. All animals in this treatment were taken down 17 days post infection, and no additional infected animals were found at take down. For *Pasteuria*, infected animals were discernable 15 days post exposure to the parasite. Remaining animals in the *Pasteuria* treatment were maintained until clearly infected or until 28 days post infection at which point infections were clearly detectable; only three additional *Pasteuria* infections were found at this date.

Section S3. Relationship between light exposure and relative infectivity in the incubation experiment.

In order to understand the impact of light environment on parasite infectivity, we analyzed the relative infectivity of light-exposed spores across the gradient of light to which they were exposed during the incubation. Light exposure depends upon light absorption in the water column by particulate and dissolved matter (more is darker), depth (deeper is darker), and season

(later is darker). We calculated within-lake light exposure for 320 nm UV and PAR separately (see Methods main text and Appendix S1).

We calculated infectivity (β) for each incubated vial (see equations S4-6 below). For relative infectivity, we divided infectivity for each light-exposed vial by the average infectivity for the corresponding dark treatment.

We assume that susceptible hosts, S, get infected as they contact spores, Z, at an infectivity, β.

$$dS/dt = - \beta S Z \quad (S4)$$

The solution to this equation is

$$S_t = S_0 \exp(- \beta Z_0 t_E) \quad (S5)$$

where S_t is the hosts remaining after exposure time t_E and exp() is the exponential function. We assume that spore concentration does not change over the exposure period, so here, Z_0 is initial dose (spores/L).

Solving for β, we obtain

$$\beta = - \ln(1 - p) / (Z_0 \ t_E) \quad (S6)$$

where p is the proportion of exposed hosts that became infected and ln is a natural log transform.

Since ln(0) is undefined, vials that had 100% infection were converted to the proportion, 0.99, for this analysis. In addition, if average infectivity in the dark (no light control) treatment was 0, the relative infectivity of the light treatment was infinite or undefined and dropped from the analysis. This was the case for 4/28 *Metschnikowia* treatments. There was one *Pasteuria* dark treatment vial (out of 83) where no exposed hosts got infected, and this vial (*Pasteuria*, dark treatment, Goodman lake, 0.5m) was dropped from this part of the analysis. Relative infectivity for the corresponding light-exposed vials was calculated with respect to the two covered vials that showed infection.

We used linear models for each parasite to test the association between averaged (by lake and depth) relative infectivity and light exposure.

Looking across lakes and seasons, relative infectivity (β) of light exposed *Pasteuria* spores declined with higher light exposure with respect to both UV ($F_{1,26}$=8.46, P=0.007; Figure S2A) and PAR ($F_{1,26}$=18.95, P<0.001; Figure S2B). Laboratory experiments indicate *Pasteuria* is sensitive to both (Overholt et al. 2020). However, since UV and PAR are correlated in our lakes, we cannot attribute declines in infectivity to either spectrum. For *Metschnikowia,* relative infectivity of light-exposed spores was not associated with UV ($F_{1,22}$=0.36, P=0.554; Figure S2C) or PAR exposure ($F_{1,22}$=2.2, P=0.153; Figure S2D); as is the case for *Pasteuria*, laboratory experiments have revealed that *Metschnikowia* is sensitive to both UV and PAR (Overholt et al. 2012). *Metschnikowia* infection rates in both light-exposed and covered treatments were low, leading to high variability and relative infectivity of light-exposed treatments greater than 1 in

some cases (when higher proportions of hosts became infected in light-exposed vials). However, the relative infectivities of most light-exposed *Metschnikowia* treatments were well below 1, indicating that light had a strong impact on spore infectivity at all levels of light exposure tested here.

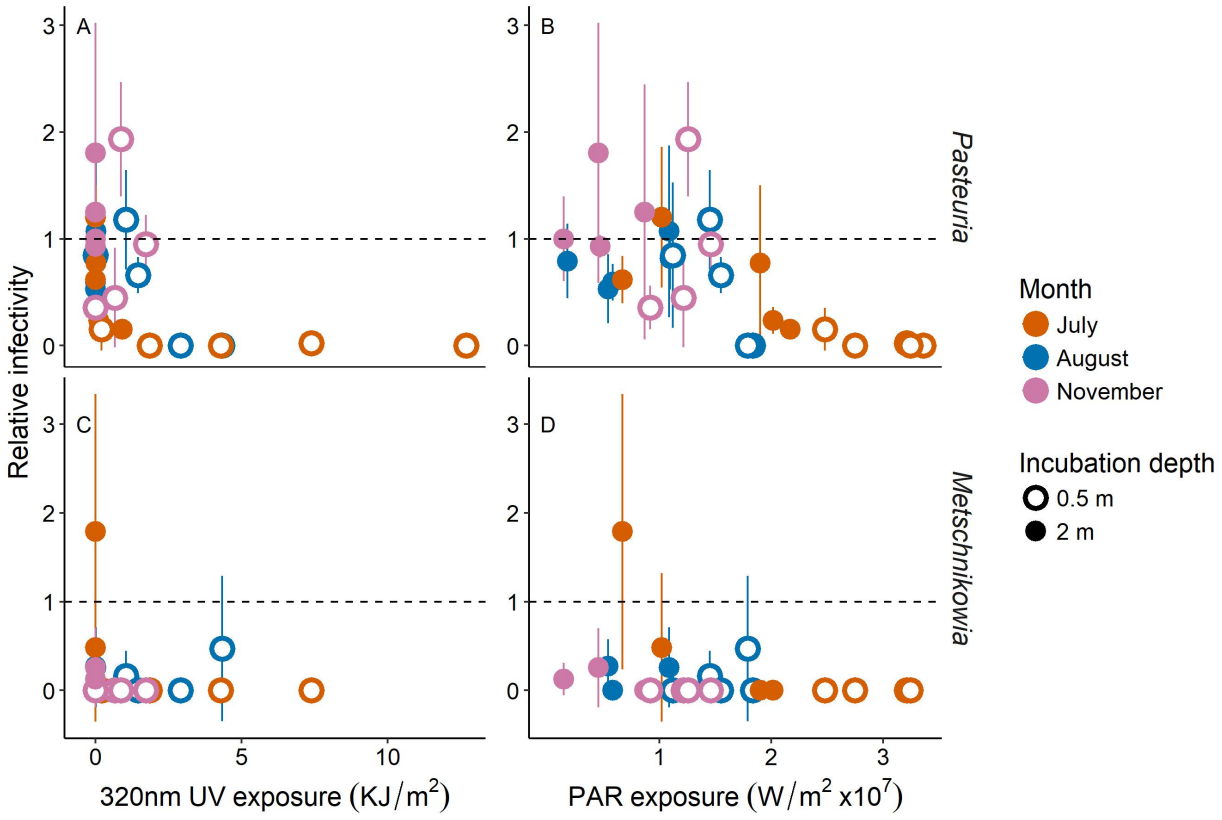

Figure S2: Relationship between relative infectivity, β, (± 1SD) and light exposure controlled by month (colors), depth (open [0.5 m] or filled [2.0 m] symbols), and lakes spread along a transparency gradient. (A, B) Greater light exposure (both UV and PAR) decreased relative infectivity of *Pasteuria* spores compared to dark treatments. (C, D) Variation in light exposure did not impact the relative infectivity of light-exposed *Metschnikowia* spores.

Section S4. Additional Field Methods

Lake Sampling

Lakes and the timing of sampling varied among years. Figure S3 shows when each lake was sampled in 2014, 2015, 2016.

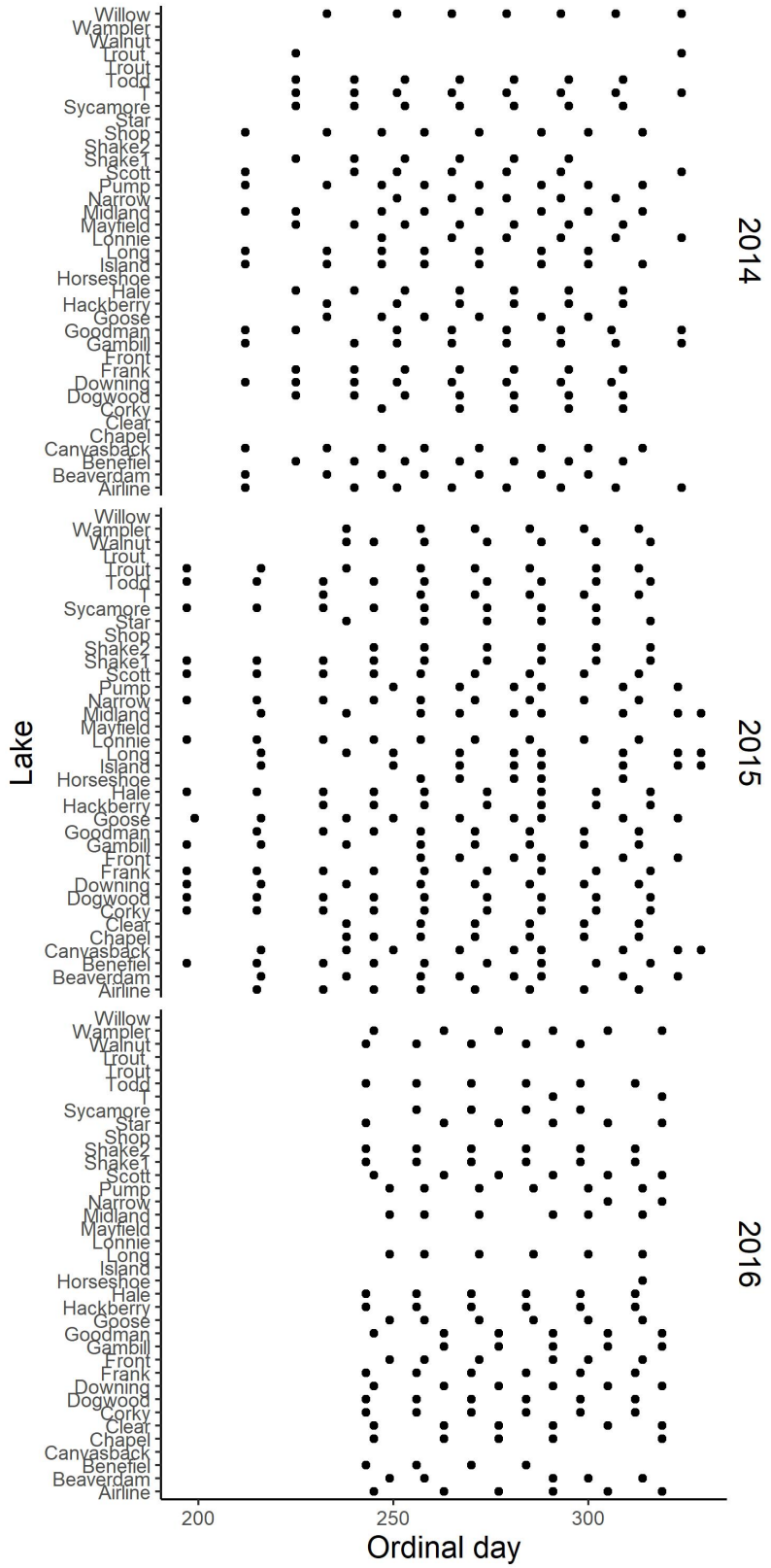

Figure S3. Sampling dates of Indiana lakes used in analysis in 2014, 2015, and 2016.

Sampling timing could affect epidemic size and start calculations. To account for potential spurious results associated with sampling timing, we checked whether variation in sampling timing was correlated with lake transparency (Fig S4). We ran a linear regression for each year with first sample date as the response variable and our index of lake transparency as a fixed effect. The first sample date was not associated with lake transparency in 2014 ($F_{1,24}$=1.60, p=0.23), 2015 ($F_{1,31}$=2.19, p=0.15), or in 2016 ($F_{1,11}$=1.58, P=0.23).

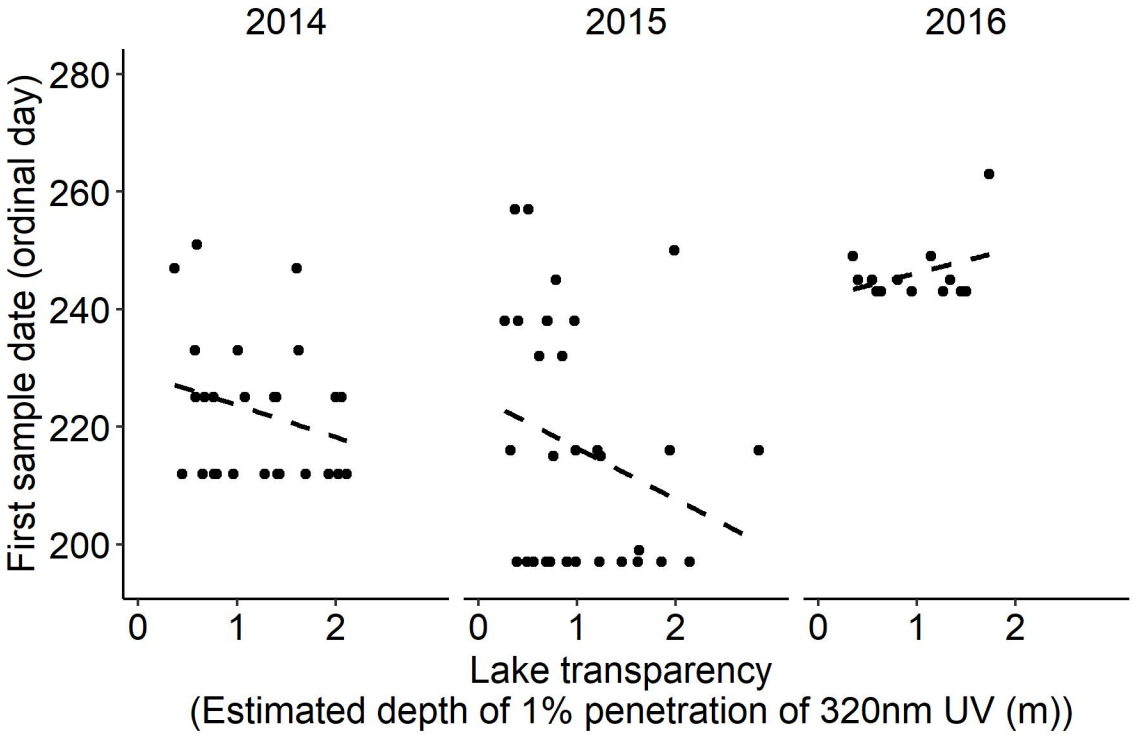

Figure S4. Association between the first sampling dates and lake transparency (depth of 1% 320 nm UV remaining). No significant associations were detected in any year of sampling (i.e., dashed trend lines).

Section S5. Differences among field models

In our analysis of maximum prevalence of each parasite, we started with a global model that included factors we believed could be important for influencing epidemic size. For *Pasteuria*, this model included our lake transparency index (see Methods), mean chlorophyll concentrations across the sampling season, mean host density across the sampling season, maximum lake depth, and year. For *Metschnikowia*, this model included an interaction between lake transparency and year, mean chlorophyll concentrations, mean host density, maximum lake depth, and epidemic start date. All predictors except year were centered and scaled. Maximum prevalence (counts of infected and uninfected animals) was modeled with binomial errors. Due to overdispersion in a binomial generalized linear model, we included an observation level random effect (Harrison et al. 2018).

We performed model selection sequentially dropping non-significant fixed effects from the global model and arriving at a model with the lowest AIC. For *Pasteuria*, this was model 5, and for *Metschnikowia*, model 3 (Figure S5). However, this process did little to alter the overall effects of the predictors that remained in the model (Figure S5).

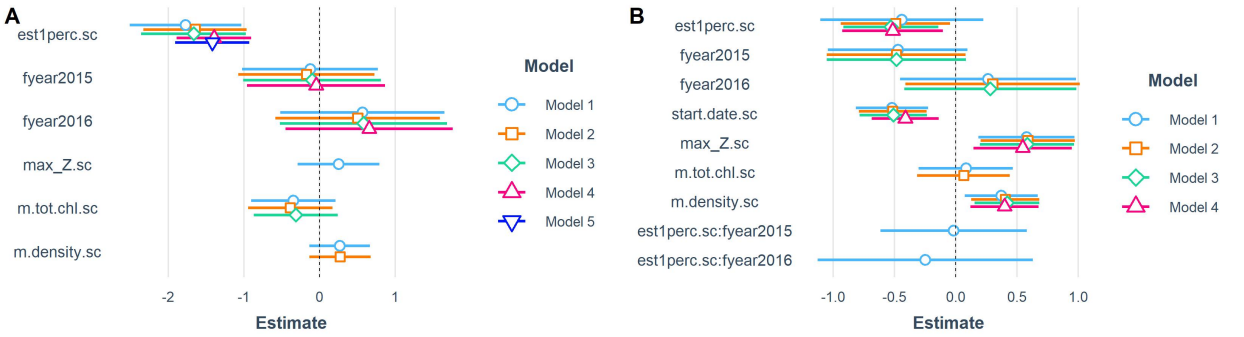

Figure S5. Effect sizes of fixed effects change little as others are removed from models of maximum prevalence of A) *Pasteuria* and B) *Metschnikowia*. Visualization of generalized linear mixed effects models (Bates et al. 2015) created by jtools (Long 2019) in R.

Appendix References

Bates, D., M. Mächler, B. Bolker, and S. Walker. 2015. Fitting linear mixed-effects models using lme4. Journal of Statistical Software 67:1–48.

Harrison, X. A., L. Donaldson, M. E. Correa-Cano, J. Evans, D. N. Fisher, C. E. D. Goodwin, B. S. Robinson, D. J. Hodgson, and R. Inger. 2018. A brief introduction to mixed effects modelling and multi-model inference in ecology. PeerJ 2018:1–32.

Kirk, J. T. O. 1993. Light and photosynthesis in aquatic ecosystems. Second edition. Cambridge University Press, Cambridge.

Long, J. A. 2019. jtools: Analysis and presentation of social scientific data. R package version 2.0.1, https://cran.r-project.org/package=jtools.

Overholt, E. P., M. A. Duffy, M. P. Meeks, T. H. Leach, and C. E. Williamson. 2020. Light exposure decreases infectivity of the *Daphnia* parasite *Pasteuria ramosa*. Journal of Plankton Research 42:41–44.

Overholt, E. P., S. R. Hall, C. E. Williamson, C. K. Meikle, M. A. Duffy, and C. E. Cáceres. 2012. Solar radiation decreases parasitism in *Daphnia*. Ecology Letters 15:47–54.

Rose, K. C., C. E. Williamson, J. E. Saros, R. Sommaruga, and J. M. Fischer. 2009. Differences in UV transparency and thermal structure between alpine and subalpine lakes: implications for organisms. Photochemical & Photobiological Sciences 8:1244.